Numerical simulation of unconstrained electron cyclotron emission

D. C. Speirs[1], K. M. Gillespie[1], K. Ronald[1], S. L. McConville[1], A. D. R. Phelps[1], A. W. Cross[1], R. Bingham[1,3], B. J. Kellett[3], R. A. Cairns[2] and I. Vorgul[2]

[1]*SUPA, Department of Physics, University of Strathclyde, Glasgow, G4 0NG, U.K.*

[2]*School of Mathematics and Statistics, University of St Andrews, St Andrews, KY16 9SS, U.K.*

[3]*Space Physics Division, STFC, Rutherford Appleton Laboratory, Didcot, OX11 0QX, U.K.*

Astrophysical radio emissions in association with plasmas having non-uniform magnetic fields have been the subject of particular interest and debate over the last thirty years [1]. Numerous such sources including planetary and stellar auroral radio emissions are spectrally well defined and exhibit a high degree of extraordinary (X-mode) polarization with frequencies of emission extending down to the local relativistic electron cyclotron frequency. In particular, for the terrestrial auroral case it is now widely accepted that such emissions are generated by an electron cyclotron-maser instability driven by a component of the precipitating auroral electron flux having a horseshoe shaped velocity distribution [2]. Such a distribution can form in the precipitating electron stream through conservation of magnetic moment in the convergent magnetic field of the polar magnetosphere and theory has shown that such distributions are unstable to cyclotron emission in the X-mode [3].

Previous work at Strathclyde concerned the numerical simulation of the electrodynamics of an electron beam subject to significant magnetic compression within a bounding waveguide structure [4,5]. Cyclotron resonant energy transfer was observed with electromagnetic modes of the waveguide at microwave frequencies, with RF conversion efficiencies of the order of 1-2%. In the current context we present the results from PiC (Particle-in-cell) code simulations of the dynamics of the cyclotron emission process in the absence of cavity / waveguide boundaries. Particular consideration was given to the convective growth rate, output spectra and RF conversion efficiencies. In all cases the 2D axisymmetric version of the finite-difference time domain PiC (Particle-in-cell) code KARAT was used. The 2D axisymmetric model allows the distribution of particles in the transverse plane of motion to be monitored via the particle population density in plots of v_θ vs v_r. This facilitates the diagnosis of cyclotron-resonant bunching effects in relative electron orbital phase. For the purpose of simulating the unbounded interaction geometry, a 44cm radius region with radially increasing

conductivity was defined around the beam propagation path. This represented an idealised absorber of electromagnetic radiation, inhibiting reflection and the formation of boundary resonant eigenmodes. An electron beam was injected into this simulation geometry with a predefined horseshoe distribution, comprising a pitch spread $\alpha = v_\perp / v_z$ of $0 \rightarrow 9.5$, beam energy of 20keV±5% and beam current of 14A. Other simulation parameters included a uniform axial magnetic flux density of 0.1T, grid resolution of 0.25cm, PiC particle merging factor of 3×10^6 electrons / PiC particle and a total simulation length (beam propagation path) of 4m.

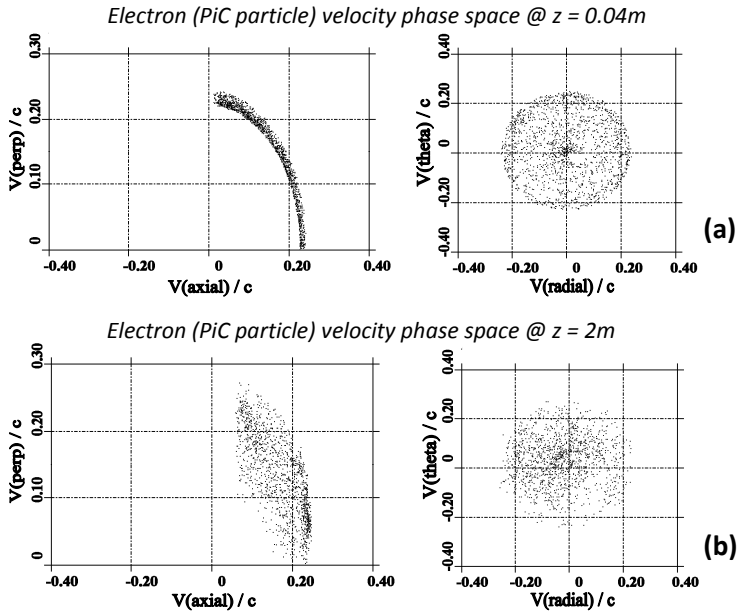

Figure 1. PiC particle velocity distributions measured on transverse planes within the simulation geometry at (a) z = 0.06m and (b) z = 2m.

Figure 1 shows the PiC particle velocity distributions at two axial positions within the unbounded simulation geometry after a 200ns run. The injected beam distribution at z = 0.04m contains a well defined pitch spread in $v_\perp$ vs v_z and no evidence of cyclotron bunching effects in the associated v_θ vs v_r plot. At an axial position of z = 2m however the picture is very different, with marked smearing in the transverse velocity profile of $v_\perp$ vs v_z over the full pitch range and evidence of electron bunching / phase-trapping in the corresponding v_θ vs v_r plot, characterised by a non uniform concentration of PiC particles extending to the origin. Both effects serve as clear evidence for beam-wave energy transfer and the action of a cyclotron maser instability.

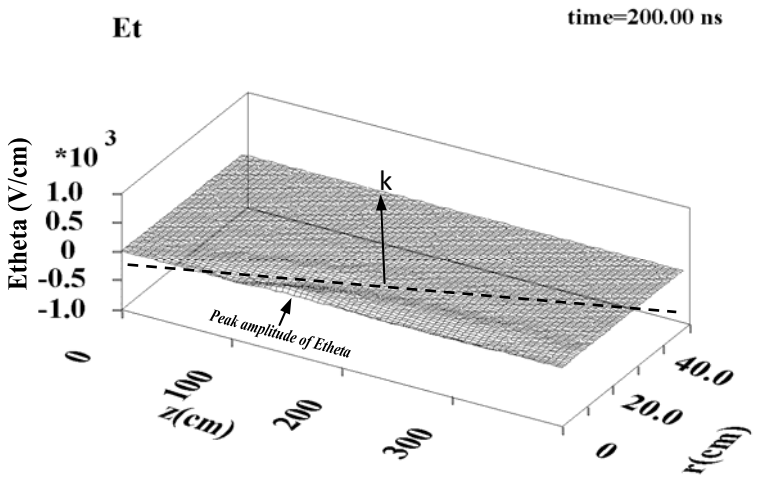

Figure 2. 3D contour plot of E_θ within the unbounded simulation geometry.

Figure 2 contains a 3D contour plot of E_θ over the simulation geometry after a 200ns run. An electromagnetic wave sourced at z ~ 1.45m is evident propagating near perpendicular to the electron beam with a small backward wave component of the wavevector. A dashed line has been superimposed parallel to the primary wavefront with an arrow indicating the corresponding orientation of the wavevector. A plot of the corresponding radial Poynting flux is presented in figure 3a measured in a plane at r = 3.5cm, over the 4m length of the simulation geometry. A DC offset is present in the measurement due to low frequency electromagnetic field components associated with the electron beam propagation. The rf output power was therefore obtained from the amplitude of the AC signal superimposed on this DC offset. A peak rf output power of ~3kW after 180ns was measured corresponding to an rf conversion efficiency of 1.1%. This is comparable to the ~1% efficiency obtained from waveguide bounded simulations [4,5] and consistent with the estimate of ~1% for the astrophysical phenomena [6,7]. The corresponding output spectrum is presented in figure 3b, showing a well defined signal at 2.68GHz. This represents a 1.1% downshift from the relativistic electron cyclotron frequency of 2.71GHz, consistent with the mild backward wave character observed in figure 2.

In conclusion, PiC simulations have been conducted to investigate the dynamics of the cyclotron emission process attributed to numerous astrophysical radio sources [1,6,7] in the absence of cavity boundaries. Computations reveal that a well-defined cyclotron emission process occurs, albeit with a low spatial growth rate compared to waveguide bounded cases [4,5]. RF output is near perpendicular to the electron beam with a slight backward-wave

character and well defined spectral output centred just below the relativistic electron cyclotron frequency. The corresponding RF conversion efficiency of 1.1% is comparable to waveguide bounded simulations [4,5] and consistent with the predictions of theory [3] and estimates of ~1% for the astrophysical phenomena [6,7].

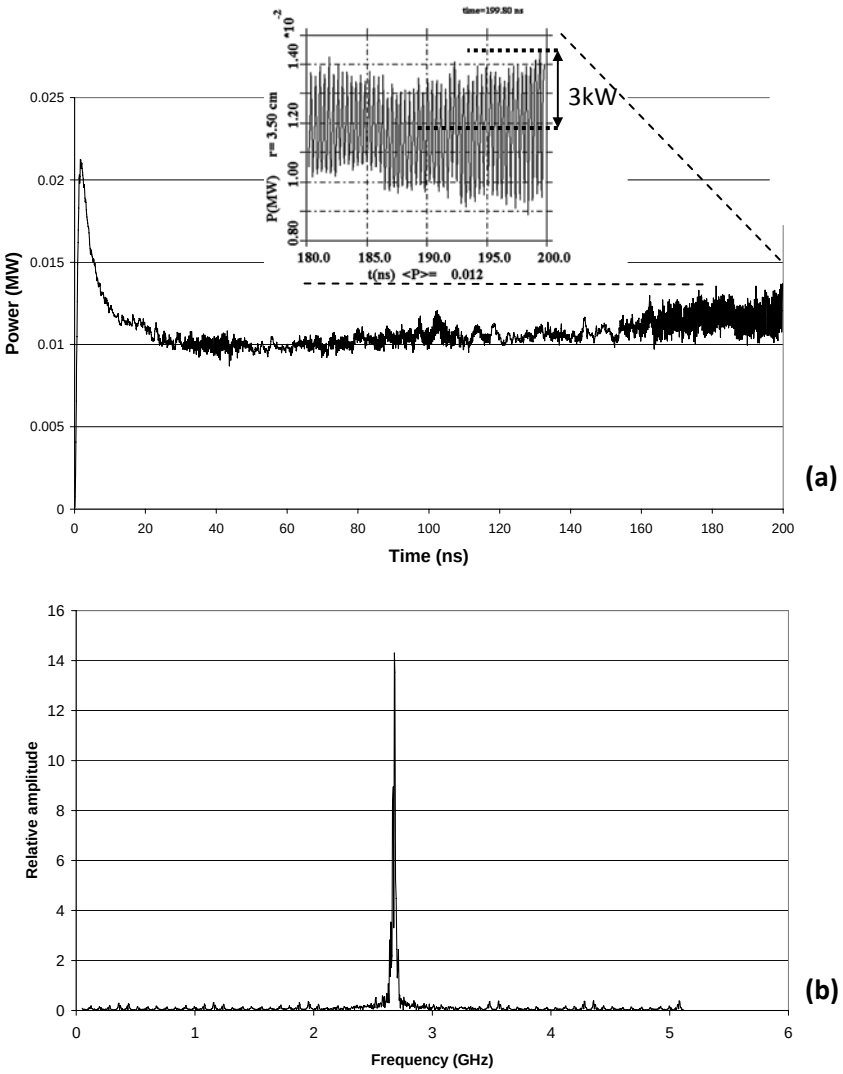

Figure 3: (a) Temporal evolution of the radial Poynting flux measured in a plane at r = 3.5cm spanning the length of the simulation. (b) Fourier transform of E_θ from t = 0 →200ns at z = 1.9m.

References

[1] A P. Zarka, Advances in Space Research, **12**, 99 (1992).
[2] D. Gurnett, "Waves in Space Plasmas", 50th Annual APS-DPP Conference (2008).
[3] R. Bingham and R. A. Cairns, Phys. Plasmas, **7**, 3089 (2000).
[4] K.M. Gillespie, D.C. Speirs, K. Ronald et al., Plasma Phys. Control. Fusion, **50**, 124038 (2008).
[5] K. Ronald, D.C. Speirs, S.L. McConville et al. Bingham, Phys. Plasmas, **15**, 056503 (2008).
[6] P.L. Pritchett and R.J. Strangeway, J. Geophys. Res., **90**, 9650 (1985).
[7] D.A. Gurnett, J. Geophys. Res., **79**, 4227 (1974).